International Journal of Pharmacy and Biological Sciences-IJPBS™ (2019) 9 (1): 1217-1227
Online ISSN: 2230-7605, Print ISSN: 2321-3272
Research Article | Biological Sciences | Open Access | MCI Approved
UGC Approved Journal

In Silico Studies towards Exploring Potential Anticancer Activity of Selected Flavonoids Against TNF-A Induced Protein 8

Meghna Somayajulu Kolluri, Shravan Kumar Gunda*, Mahmood Shaik
Division of Bioinformatics, PGRRCDE, Osmania University, Hyderabad – 500007

Received: 10 Oct 2018 / Accepted: 8 Nov 2018 / Published online: 1 Jan 2019
Corresponding Author Email: gunda14@gmail.com

Abstract
TNFAIP8 is a cytosolic anti-apoptotic and oncogenic protein found mainly and cancerous cells. It contributes to carcinogenesis by promoting proliferation and autophagy, thus improving cancer cell survival. Therefore, it is a suitable therapeutic target for cancer treatments and gene therapy. In this study, 3-Dimensional structure of Tumor necrosis factor alpha-induced protein 8 from Homo sapiens was described by Homology modeling method based on the template protein of Chain A, Crystal Structure of Tipe2 from Homo sapiens and selected natural flavonoids as ligands were docked to the active site of modelled protein. The quality of the 3-Dimensional structure of the generated model was confirmed by various validation tools. The generated model exhibited 96.3% of amino acid residues in most favored region. Molecular docking study showed that the all the compounds exhibited good binding energy than already existing drugs. Compound 7-O-methyl naringenin exhibited highest binding energy of -6.36 Kcal/mol.

Keywords
Homology modelling, Molecular Docking, TNF-α, Natural flavonoid Compounds

*****

INTRODUCTION:
Tumor necrosis factor α-induced protein 8 (TNFAIP8), also known as SCC-S2/GG2-1/NDED, is a 21kDa cytosolic anti-apoptotic and oncogenic protein. It is highly expressed in many cancer cell lines such as MOLT4, K562, A549, and SKOV-3 etc. and its expression is confined to the cytoplasmic compartment of tumor cells. Its expression is confined to the cytoplasmic compartment of tumor cells[1,2]. It is also considered a risk factor in Hodgkin's lymphoma[3]. Overexpression of this protein occurs in the presence of TNF- α and by the action of NF-κB in many cells and results in cell proliferation and enhanced cell survival. The death effector domain DED present in the protein causes inhibition of caspase-3 and caspase-8 activity leading to apoptosis[2,4,5]. TNF- α treatment was also previously shown to induce autophagy and apoptosis in JEG-3[6] and L929 cells which was enhanced with inhibition of the NF-κB pathway[7].
TNFAIP8 has a role as a regulator of apoptosis while promoting autophagy to enhance the survival of cancer cells. Studies show that TNFAIP8 knockouts exhibit reduced proliferation and increased apoptosis by interfering with other proteins involved in such processes. TNFAIP8 was found to regulate

expression of cell cycle proteins like cyclin D1 and CD K6, therefore arresting the cell cycle between G1 and S phase with a decreased percentage of cells in the S phase[1,8]. However, TNFAIP8 KO's of osteosarcoma cells caused cell cycle arrest at the G0/G1 boundary while increasing the apoptotic rate in Saos-2 and U2OS cells[9]. In thymocytes, overexpression of TNFAIP8 increases apoptosis by increasing their sensitivity to glucocorticoids resulting in glucocorticoid-mediated apoptosis[4]. KO's also show the expression of genes associated with proliferation suppression and apoptosis[10]. Overexpression also shows aggressive phenotypes such as large tumor types and higher recurrence[8].

Many studies have identified TNFAIP8 v2 (variant 2) as a contributor to carcinogenesis by broadly suppressing p53 activity, thus interfering with p53-dependent tumor suppression. Variant 2 expression is p53 independent and high in many cancer cell lines. Overexpression of v2 is associated with decreased binding with target proteins and p53 activity. TNFAIP8 v2 depleted cells exhibited defective DNA synthesis and cell cycle arrest at the S-phase along with increased levels of cyclin D1, E1 and E2[11]. These findings supported the importance of TNFAIP8 v2 in cancer cell survival and progression.

In NSCLC, TNFAIP8 expression levels were high in tumor cells but low in tumor-infiltrating CD4+ and CD8+ T cells which continued to decrease as the cancer progressed[12]. Depletion of TNFAIP8 expression with small interfering RNA inhibited growth and invasion in lung cell lines[13]. As TNFAIP8 expression largely is associated with tumor cell survival and proliferation, it is used a marker for prognosis in cancer patients. High levels of expression generally indicate poor prognosis and survival rate and high TNFAIP8 levels indicate metastasis to lymph nodes, advanced pT stage and advanced TNM staging[10,13]. Treatment with cationic liposomal formulation of antisense TNFAIP8 oligo in athymic mice resulted in decreased pulmonary metastasis and SCC-S2 expression *in vivo.* This also led to the down regulation of known metastasis proteins MMP-1 and MMP-9[14]. The findings make TNFAIP8 an ideal therapeutic target in cancer treatments and gene therapy.

The aim of present study was to construct 3D model of O95379_HUMAN[15] and explore the binding interactions of natural flavonoid compounds through molecular docking studies. Homology Modelling or comparative modelling of proteins refers to the construction of an atomic model of the chosen protein based on a template protein with which it shares similarity. In this process, only those templates that show sequence similarities with that of the protein are chosen to obtain a model that most closely resembles that of the template.

Molecular docking is a structure-based drug designing tool used to produce ligands with specific electrostatic and stereochemical attributes to achieve a higher binding efficiency. It is a key tool in structural molecular biology and computer assisted drug design[16-18]. It aims to predict affinity between proteins and ligands at the receptor target site. With the discovery of new proteins and ligands, it becomes important to study the various protein-ligand and protein-protein interactions to better understand cell dynamics. Docking tools have had a great impact in the study of such interactions[18]. This is achieved through pose prediction, virtual screening, and binding affinity prediction. In these steps, the possible ligand conformations are generated with respect to the receptor binding site and the subsequent physical and chemical molecular interactions are predicted[16]. Numerous possible 'poses' are tried and evaluated. The scoring function assigns poses with their lowest binding energy is selected as the best match or binding mode, as it is the most stable of the poses[17]. The energy values reflect the affinity between the given ligand and its receptor binding site. Thus, a good scoring function can distinguish between active and inactive ligands and identify the most potent ligands.

From ancient to modern times, plants and other herbs have been used as medicinal agents[19] Natural products or natural compounds and their derivatives as chemotherapeutic agents, including plant-derived antimalarial, antifungal, antitumor, antiviral, anticancer, antidiabetic, antialzheimers, antiarthritic, antiinflammatory agents etc., Herbal medicine is the primary source of new lead compounds. Maximum of the plants contains polyphenols, flavonoids, alkaloids, tannins, saponins, terpenoids, lignans, sterols, ididoids, fatty acids etc.

METHODOLOGY

Sequence alignment and structure prediction

The amino acid sequence of Tumor necrosis factor alpha-induced protein 8 (Uniprot accession number: O95379) from the species Homo sapiens was retrieved from the UniProtKB database (http://www.uniprot.org/). A BLAST (Basic Local Alignment Search Tool) search was performed to select the template and resulted with the best match Crystal structure of Chain A, Crystal Structure Of Tipe2 from Homo sapiens (PDB ID: 3F4M_A)[20] with 53% similarity having a resolution of 1.70 Å making it an excellent template. The three-dimensional

structure was generated using Modeller 9.20. The respective templates are retrieved from protein databases like PDB[21,22]. When choosing the template, it is important to consider the sequence identity and resolution of the template. When both parameters are high the resulting model would be sufficiently good to allow structural and functional research[23].

The final validation of the model was performed using PROCHECK for Ramachandran plot. The RMSD (root mean square deviation) was calculated by superimposing (3F4M) over the generated model to access the accuracy and reliability of the generated model. Sequence alignment of TNF-α induced protein 8 and template

```
CLUSTAL O(1.2.4) multiple sequence alignment


sp|O95379|TFIP8_HUMAN      MHSEAEESKEVATDVFNSKNLAVQAQKKILGKMVSKSIATTLIDDTSSEVLDELYRVTRE 60
pdb|3F4M|A                 ------------------------------------RSVAHLFIDETSSEVLDELYRVSKE 25
                                                               :*:*  :**:************::*

sp|O95379|TFIP8_HUMAN      YTQNKKEAEKIIKNLIKTVIKLAILYRNNQFNQDELALMEKFKKKVHQLAMTVVSFHQVD 120
pdb|3F4M|A                 YTHSRPQAQRVIKDLIKVAIKVAVLHRNGSFGPSELALATRFRQKLRQGAMTALSFGEVD 85
                           **:.: :*:::**:***..**:*:*:**..*. .****  :*::*::* ***.:** :**

sp|O95379|TFIP8_HUMAN      YTFDRNVLSRLLNECREMLHQIIQRHLTAKSHGRVNNVFDHFSDCEFLAALYNPFGNFKP 180
pdb|3F4M|A                 FTFEAAVLAGLLTECRDVLLELVEHHLTPKSHGRIRHVFDHFSDPGLLTALYGP--DFTQ 143
                           :**:  **: **.***::* :::::*** *****:.:******* :*:***.* :*.

sp|O95379|TFIP8_HUMAN      HLQKLCDGINKMLDEENI   198
pdb|3F4M|A                 HLGKICDGLRKLLDEGKL   161
                           ** *:***:.*:*** ::
```

Figure 1: Sequence alignment of query TNF-α induced protein 8 and template 3F4M by clustalW

MODELLER 9.20 was then used to gain satisfactory models; an automated approach to homology modeling by satisfaction of spatial restrains. Sequence alignments using the protein and template sequences is then carried out using platforms like ClustalX or ClustalW[24]. Homology models for the chosen protein are then constructed using modeller programs like Modeller 9.20[25]. After manually modifying the alignment input file in MODELLER 9.20 to match the query and template sequence, 20 models were generated. The best model is determined by the lowest value of the Modeller Objective Function. The stereochemical quality of the given models is then evaluated using softwares like PROCHECK[26] and the model can be used for further structural or functional study. Ramachandran plot explains residue by residue listing facilitates, the in-depth calculation of Psi/Phi angles and the backbone conformation of the models.

Docking methodology

The ten natural flavonoid derivatives were downloaded from NCBI and saved it into. mol2 format. Molecular Docking study was performed to all the natural flavonoid molecules separately by using AutoDock4.2 program, using the Lamarckian Genetic Algorithm (LGA) and implemented empirical free energy function. Initially, the modelled Tumor necrosis factor alpha-induced protein 8 protein was loaded, and hydrogen were added and saved it in PDBQT format. Later the ligand was loaded and set conformations and saved it in PDBQT format. The grid parameters were selected and calculated using AutoGrid. For all the dockings, a grid-point spacing of 0.375 Å was applied and grid map with 60×60×60 points were used. Active site was predicted in Sybyl6.7 biopolymer module. X, Y, Z Coordinates were selected on the basis of the amino acids present in the active site. Default parameters were used to run the Autodock.

Results and Discussion:

Homology modelling and model evaluation:

The present study reports that the template protein (PDB ID: 3F4M) having high degree of homology with O95379 protein was used as a template with good atomic resolution of its crystal structure. The target sequence of Tumor necrosis factor alpha-induced protein 8 (uniprot accession number: O95379) from Homo sapiens having 198 amino acid residues was retrieved from the uniprot protein sequence database with Accession No. O95379. PDB Id 3F4M was identified and selected as template using BLAST having 53% identity. The structure was modelled using modeller9.20. The generated structure was validated using Protein Structure and by PROCHECK. The generated model showed 96.3% of amino acid residues in core region, 3.7% of amino acid residues in additionally allowed region, there is no amino acids present in generously allowed region and disallowed region. The template PDB shows 97.8% of amino acids in core region, 2.2% of the amino acid residues in additionally allowed region and there is no amino acid residues in generously and disallowed region. Cartoon model of the modelled protein and

Ramachandran plot of the modelled protein are shown in figure.2 and figure.3. RMSD was calculated for template and generated model by using SPDBV. Both the models were loaded and superimposed using carbon alpha and calculated RMSD. It showed RMSD of 0.21Å, which indicates the generated model shows similar function as template. Superimposed query and template model is displayed in figure 4.

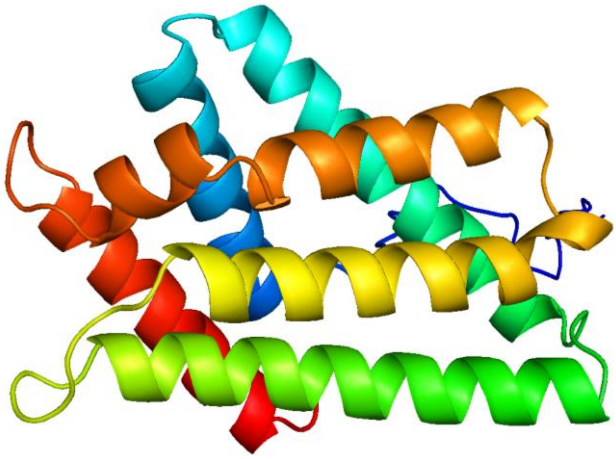

Figure 2: Cartoon model of Homology derived TNF-α induced protein 8

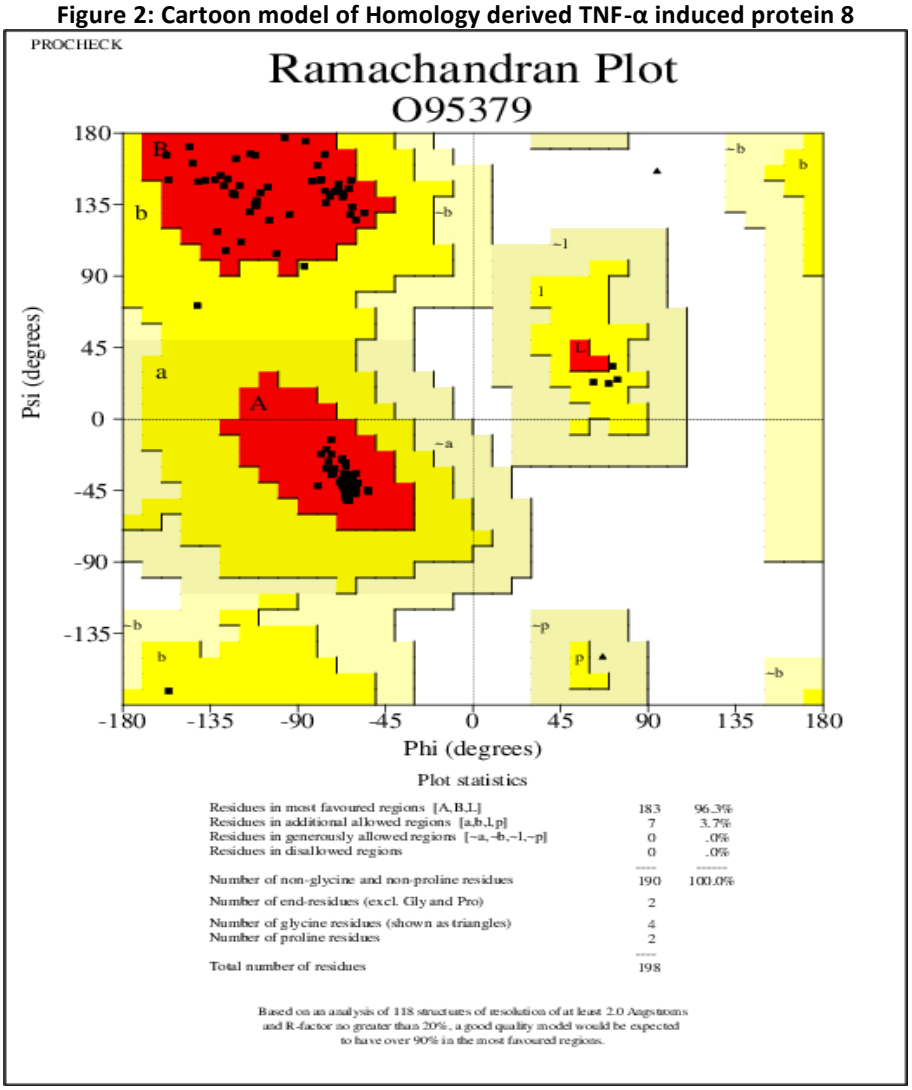

Figure 3: Ramamchandran plot analysis of the modeled TNF-α induced protein 8 structure.

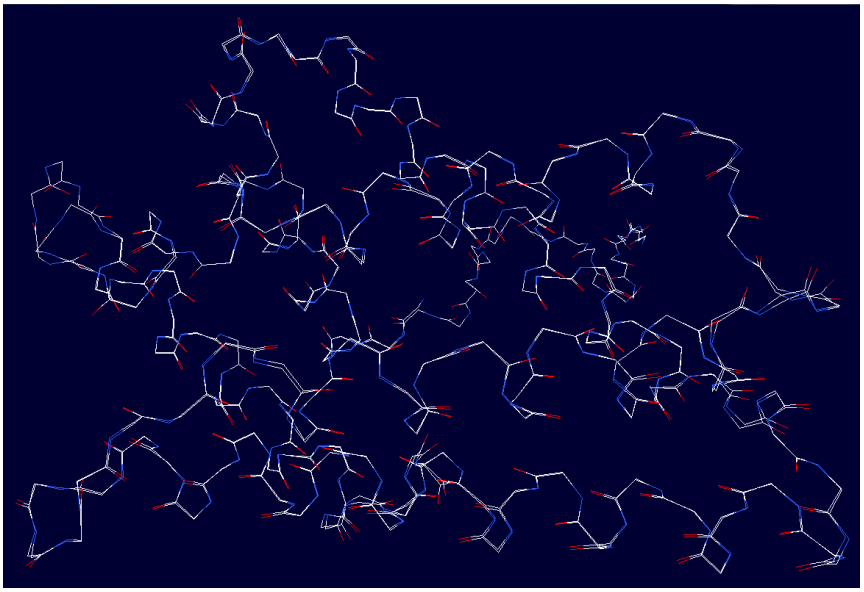

Figure 4: Superimposed model of TNF-α induced protein 8 and Template 3F4M

Molecular docking results

Identification of active site pockets. The active site prediction was carried out using Tripo's Sybyl6.7. It showed three active site pockets. The amino acids which are present in pocket one are Leu128, Leu132, Phe162, Phe167, Leu168, Leu182, Leu185, Ile189, Val113, and amino acids present in the pocket two and three are Met138, Ile142, Leu82, Phe91, Leu96, Leu98, Met99 and Tyr172, Phe116, Phe123 respectively. These are used to identify best ligand binding site of the protein.

Molecular docking is the most extensively used method for the calculation of protein-ligand interactions. It is an efficient method to predict the potential ligand interactions. In this study, the native plant secondary metabolites (ligands) have been identified as potent TNF-α inhibitors. All the compounds exhibit good biological activity properties. All the flavonoid compounds were then further analyzed to identify their best docking score and docking pose. These studies revealed that the most interacting residues in the active site of TNF-α induced protein.

AutoDock4.2 uses binding free energy assessment to assign the best binding conformation**.** Twenty potent flavonoid molecules were docked individually. Further, docking experiments of some selective potent molecules allowed us to compare the activity of docked molecules to **standard drugs as controls**. However, the compound 7-O-methyl naringenin and compound Diadzein for modelled protein have some collective structural features, the molecule shows interactions and better lower free energy values, indicating more thermodynamically favored interactions.

Specifically, compound 7-O-methyl naringenin exhibited the highest binding energy of value -6.36 K.cal/mol with Tyr172 when compared to the standard drugs Celecoxib, Diclofenac, Indomethacin exhibited binding energy of -5.48 Kcal/mol, -3.60 Kcal/mol and -5.13 Kcal/mol respectively. Diadzein exhibited binding energy of -6.28 K.cal/mol with interacting Tyr172. Eight compounds are interacting with Glu60, seven compounds are interacting with Asn177 and three compounds are interacting with Tyr172. All the compounds exhibited good binding energy are shown in Table 1 and protein ligand interactions are shown in figure 5. All the flavonoid compounds exhibited high binding energy than Celecoxib, Diclofenac, and Indomethacin. Interestingly, all the docked compounds exhibited high binding or closer energy values compare to the Celecoxib, Diclofenac, Indomethacin (Table 2) and the interaction diagrams shown in (Fig6). Finally, Celecoxib, Diclofenac, Indomethacin showed a lesser binding energy of -5.48 Kcal/mol, -3.60 Kcal/mol and -5.13 Kcal/mol when compare to binding energy of compound 7-O-methyl naringenin with -6.36 Kcal/mol.

S.No	Interacting amino acids	Binding energy ΔG (Kcal/Mol)	Dissociation Constant (kI) (µM)
7,4'-O-dimethoxy-5-hydroxy-flavone	Asn177, Glu60	-5.49	94.72
7-O-methoxy-4',5-hydroxy-flavone	Asn177, Glu60	-5.52	90.31
7-O-methyl naringenin	Tyr172	-6.36	21.9
3,5,7-hydroxy-3,4'-methoxy 6-8 methyl flavone	Asn177, Tyr61	-5.74	62.01
Apigenin	Phe159	-5.95	43.6
BiochaninA	Glu166, Tyr61	-5.56	84.47
Diadzein	Tyr172	-6.28	24.99
Genistein	Tyr172	-5.65	72.34
Hesperetin	Gln63, Asn177, Thr62, Glu60	-5.50	93.51
Casticin	Asn177, Glu60, Tyr61	-5.61	77.19
Genkwanin	Asn177, Glu60	-5.49	93.87
Chaplashin	His16, Asp160, Glu166	-6.11	33.12
Chrysospenol D	Glu60	-5.06	193.84
Cudraflavone B	Glu60	-6.08	34.9
CudraflavoneC	Glu166, Tyr61	-5.51	91.82
Eriodictyol	Asn177, Gln63, Glu60, Thr62	-5.20	155.28
GlepidotinA	Glu60, Glu166	-5.71	64.72
Morusin	Thr62, GLU166	-6.13	32.33
Chrysin	Phe159	-6.22	27.66
Artemetin	His161	-5.56	83.42

Table 1: Intermolecular Hydrogen bonds between selected flavonoids with modelled TNF-α induced protein.

Standard drugs

S. No.	Interacting amino acids	Binding energy ΔG (Kcal/Mol)	Dissociation Constant (kI) (µM)
Celecoxib	Glu60	-5.48	95.39uM
Diclofenac	Arg125, Asn173	-3.60	2.31mM
Indomethacin	Gln63	-5.13	173.74uM

Table 2: Intermolecular Hydrogen bonds between selected contorls with TNF-α induced protein.

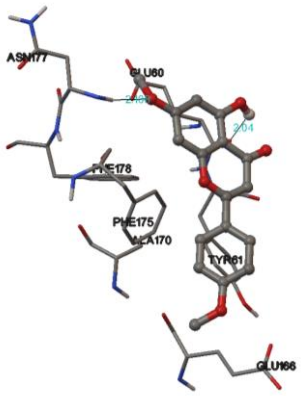

1

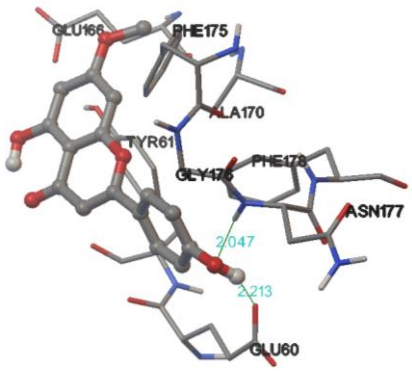

2

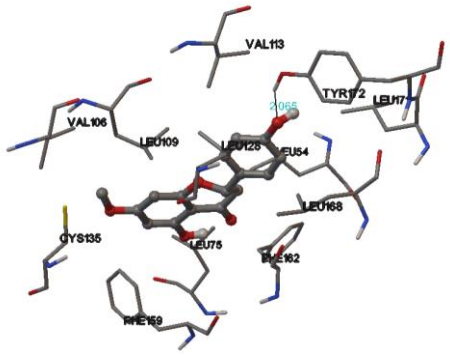
VAL113
TYR172
LEU171
VAL106
LEU109
LEU128
LEU54
LEU168
CYS135
LEU75
PHE162
PHE159

3

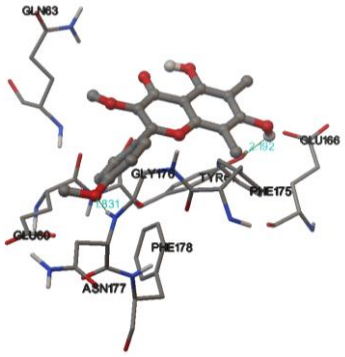
GLN63
GLU166
GLY176
TYR61
PHE175
GLU60
PHE178
ASN177

4

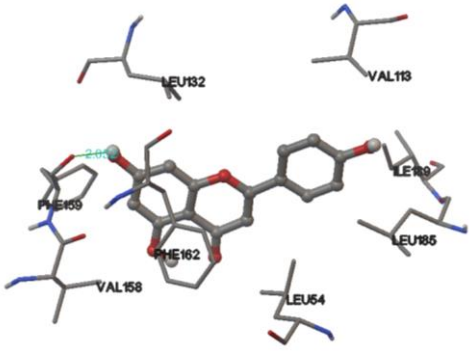
LEU132
VAL113
PHE159
LEU185
PHE162
VAL158
LEU54

5

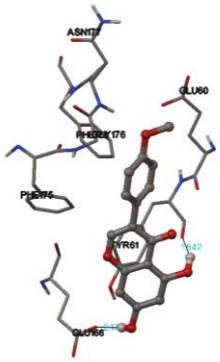
ASN177
GLU60
PHE176
PHE175
TYR61
GLU166

6

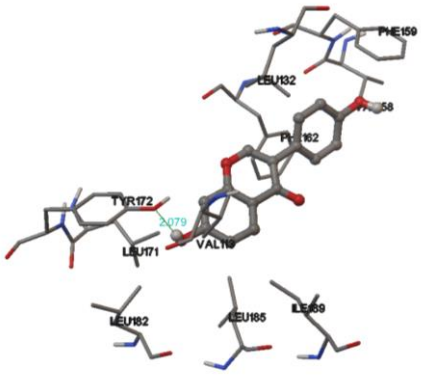
PHE159
LEU132
TYR172
LEU171
LEU182
LEU185

7

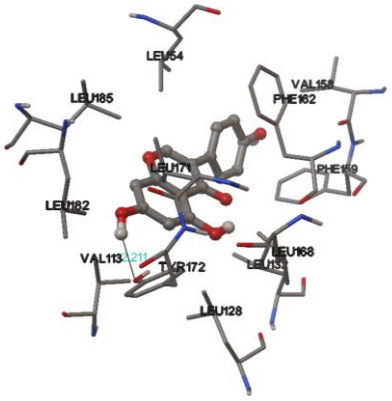
LEU54
LEU185
VAL158
PHE162
LEU171
PHE159
LEU182
VAL113
TYR172
LEU168
LEU128

8

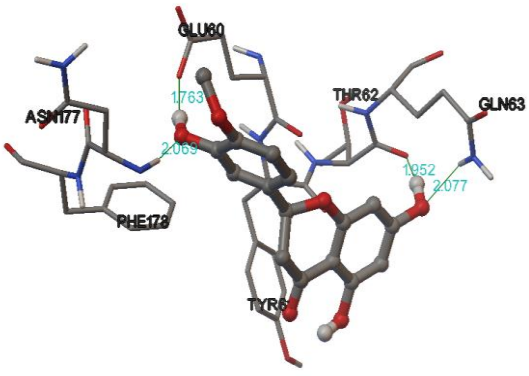
GLU60
THR62
GLN63
ASN177
PHE178
TYR61

9

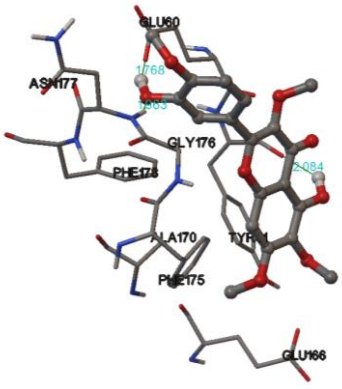
GLU60
ASN177
GLY176
PHE178
ALA170
TYR61
PHE175
GLU166

10

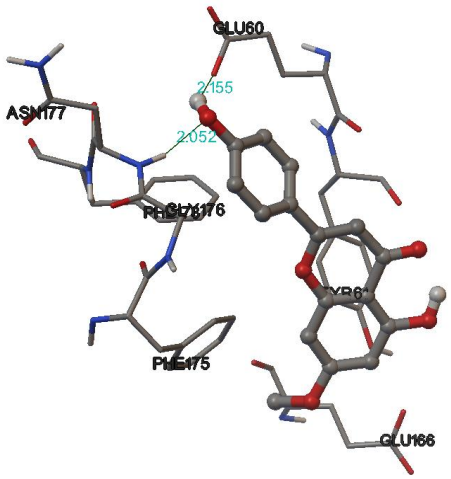

11

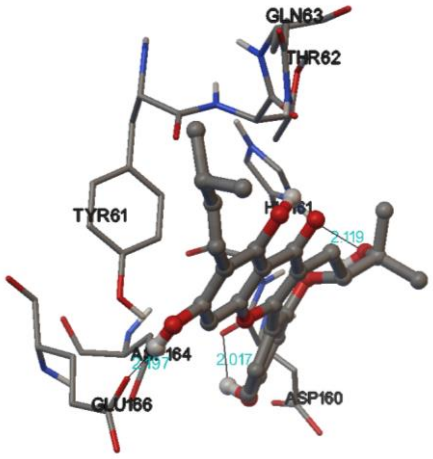

12

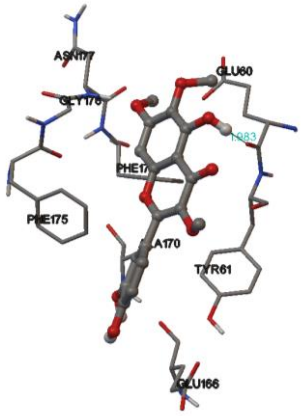

13

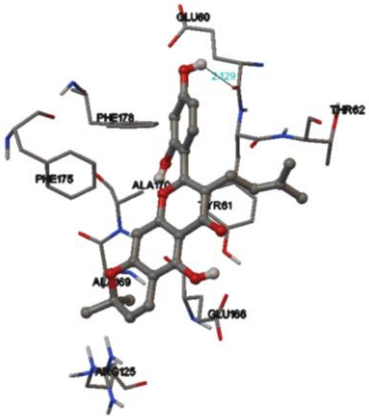

14

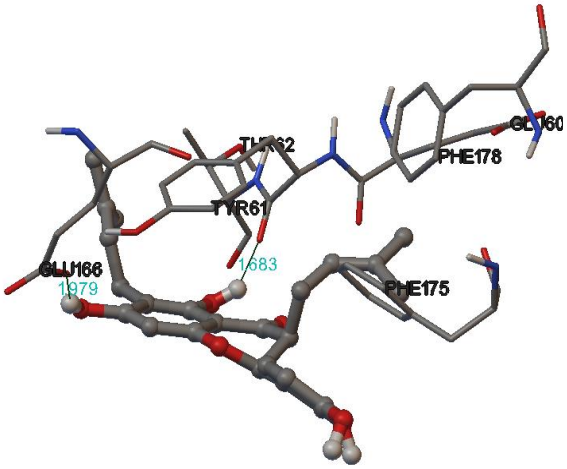

15

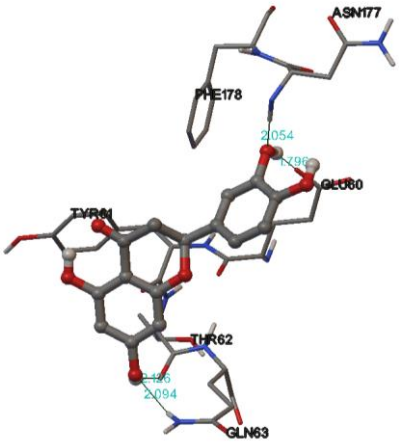

16

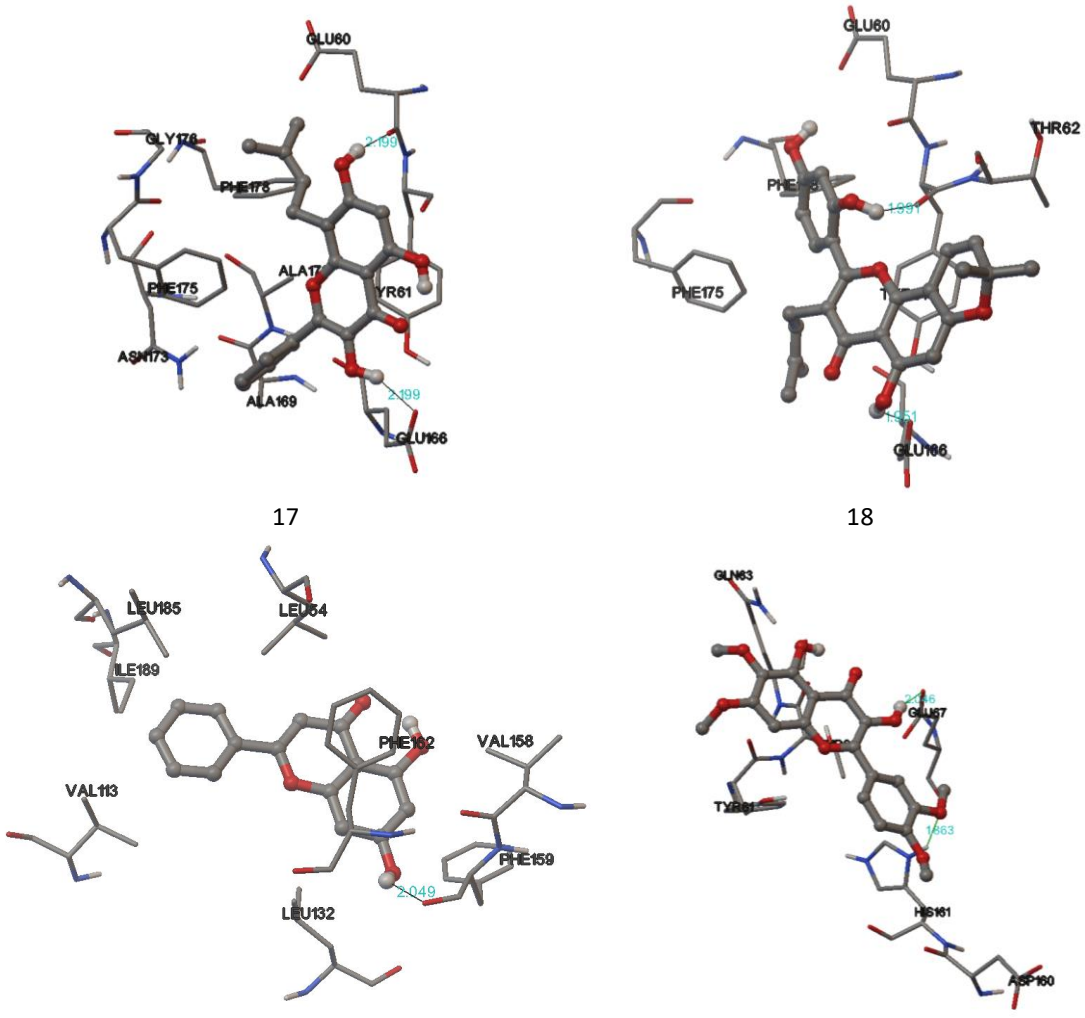

17 18

19 20

Figure 5: Docking result of the twenty flavonoids against TNF-α induced protein 8

Standard drugs

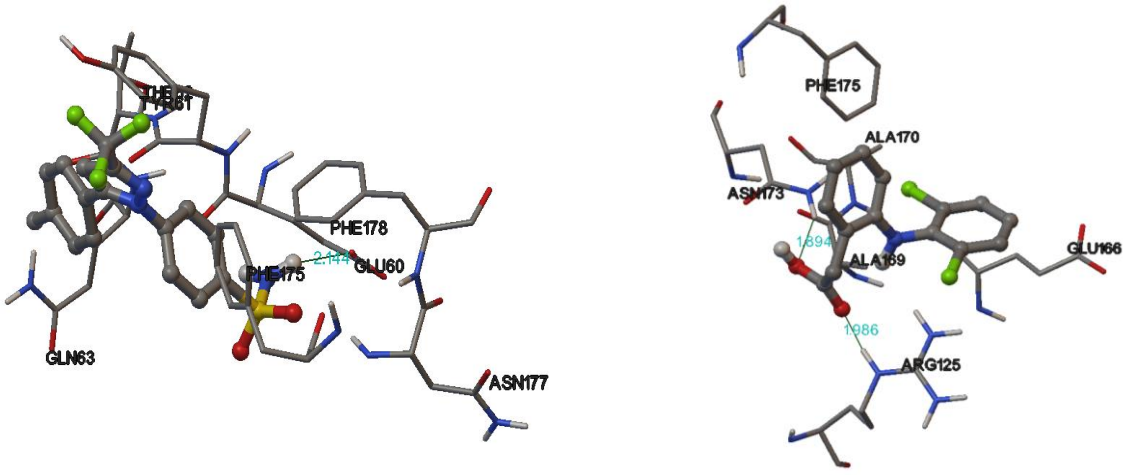

1 2

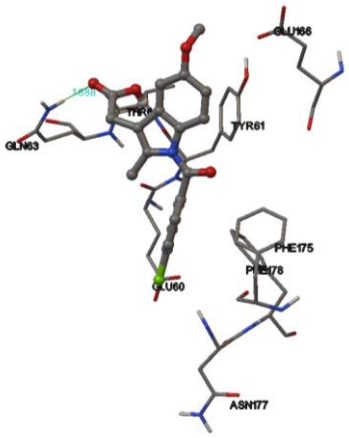

3

Figure 6: Docking result of the three control drugs against TNF-α induced protein 8

CONCLUSION:

Tumor necrosis factor alpha-induced protein 8 is a potential target for oncogenic and anti-apoptotic protein. Our present study provided the 3-Dimensional structure of TNFAIP8 through a homology modeling method. The model showed 96.3% of amino acid residues in core region and molecular docking studies were also showed very good binding energies and interactions when compared to satandard drugs. Compound 7-O-methyl naringenin exhibited the highest binding energy of value -6.36 K.cal/mol with Tyr172. The statistics of modelled protein and template protein is similar in crystal structure. This proves that natural flavonoids as potent inhibitors for cancer. These compounds can be tested further in the future against this target protein.

REFERENCES:

1. Xing Y, Liu Y, Liu T, Meng Q, Lu H, Liu W, et al., TNFAIP8 promotes the proliferation and cisplatin chemoresistance of non-small cell lung cancer through MDM2/p53 pathway. Cell Commun Signal, 16 (1): 43, (2018)
2. Liu T, Gao H, Chen X, Lou G, Gu L, Yang M, et al., TNFAIP8 as a predictor of metastasis and a novel prognostic biomarker in patients with epithelial ovarian cancer. Br J Cancer, 109 (6): 1685-1692, (2013)
3. Porturas TP, Sun H, Buchilis G, Lou Y, Liang X, Cathopoulis T et al., Crucial roles of TNFAIP8 protein in regulating apoptosis and Listeria infection. J Immunol, 194 (12): 5743-5750, (2015)
4. Woodward MJ, de Boer J, Heidorn S, Hubank M, Kioussis D, Williams O, et al., Tnfaip8 is an essential gene for the regulation of glucocorticoid-mediated apoptosis of thymocytes. Cell Death Differ, 17 (2): 316-323, (2010)
5. Kumar D, Whiteside TL, Kasid U., Identification of a Novel Tumor Necrosis Factor-alpha-inducible Gene, SCC-S2, Containing the Consensus Sequence of a Death Effector Domain of Fas-associated Death Domain-like Interleukin-1beta-converting Enzyme-inhibitory Protein. J Biol Chem, 275 (4): 2973-2978, (2000)
6. Cha HH, Hwang JR, Kim HY, Choi SJ, Oh SY, Roh CR., Autophagy Induced by Tumor Necrosis Factor α Mediates Intrinsic Apoptosis in Trophoblastic Cells. Reprod Sci, 21 (5): 612-622, (2014)
7. Ye YC, Yu L, Wang HJ, Tashiro S, Onodera S, Ikejima T., TNFα-Induced Necroptosis and Autophagy via Supression of the p38–NF-κB Survival Pathway in L929 Cells. J Pharmacol Sci, 177 (3): 160-169, (2011)
8. Dong Q, Fu L, Zhao Y, Xie C, Li Q, Wang E., TNFAIP8 interacts with LATS1 and promotes aggressiveness through regulation of Hippo pathway in hepatocellular carcinoma. Oncotarget, 8 (9): 15689-15703, (2017)
9. Zhou Z, Li Z, Shen Y, Chen T., MicroRNA-138 directly targets TNFAIP8 and acts as a tumor suppressor in osteosarcoma. Exp Ther Med, 14 (4): 3665-3673, (2017)
10. Niture S, Ramaling M, Kedir H, Patacsil D, Niture SS, Li J et al., TNFAIP8 promotes prostate cancer cell survival by inducing autophagy. Oncotarget, 9 (42): 26884-26899, (2018)
11. Lowe JM, Nguyen TA, Grimm SA, Gabor KA, Peddada SD, Li L, et al., The novel p53 target TNFAIP8 variant 2 is increased in cancer and offsets p53-dependent tumor suppression. Cell Death Differ, 24 (1): 181-191, (2017)
12. Wang L, Song Y, Men X., Variance of TNFAIP8 expression between tumor tissues and tumor-infiltrating CD4+ and CD8+ T cells in non-small cell lung cancer. Tumour Biol, 35 (3): 2319-2325, (2014)
13. Dong QZ, Zhao Y, Liu Y, Wang Y, Zhang PX, Jiang GY et al., Overexpression of SCC-S2 correlates with lymph node metastasis and poor prognosis in patients with non-small-cell lung cancer. Cancer Sci, 101 (6): 1562-1569, (2010)
14. Zhang C, Chakravarty D, Sakabe I, Mewani RR, Boudreau HE, Kumar D, et al., Role of SCC-S2 in

Experimental Metastasis and Modulation of VEGFR-2, MMP-1, and MMP-9 Expression. Mol Ther, 13 (5): 947-955, (2006)
15. https://www.uniprot.org/uniprot/O95379
16. Guedes IA, de Magalhães CS, Dardenne LE., Receptor–ligand molecular docking. Biophys Rev, 6 (1): 75-87, (2014)
17. Huang SY, Zou X., Advances and Challenges in Protein-Ligand Docking. Int J Mol Sci, 11 (8): 3016-3034, (2010)
18. Ramirez D, Caballero J., Is It Reliable to Use Common Molecular Docking Methods for Comparing the Binding Affinities of Enantiomer Pairs for Their Protein Target? Int J Mol Sci, 17 (4): 525, (2016)
19. Kuo-Hsiung Lee., Current Developments in the Discovery and Design of New Drug Candidates from Plant Natural Product Leads. J. Nat. Prod, 67: 273-283, (2004)
20. https://blast.ncbi.nlm.nih.gov/Blast.cgi#aInHdr_225698051
21. Yadav S, Pandey SK, Singh VK, Goel Y, Kumar A, Singh SM., Molecular docking studies of 3- bromopyruvate and its derivatives to metabolic regulatory enzymes: Implication in designing of novel anticancer therapeutic strategies. PLoS One, 12 (5): e0176403, (2017)
22. Kumbhar BV, Borogaon A, Panda D, Kunwar A., Exploring the Origin of Differential Binding Affinities of Human Tubulin Isotypes aßII, aßIII and aßIV for DAMA-Colchicine Using Homology Modelling, Molecular Docking and Molecular Dynamics Simulations. PLoS One, 11 (5): e0156048, (2016)
23. Jiang ZY, Chu HX, Xi MY, Yang TT, Jia JM, Huang JJ, et al., Insight into the Intermolecular Recognition Mechanism between Keap1 and IKKß Combining Homology Modelling, Protein-Protein Docking, Molecular Dynamics Simulations and Virtual Alanine Mutation. PLoS One, 8 (9): e75076, (2013)
24. Saxena AK, Devillers J, Bhunia SS, Bro E., Modelling inhibition of avian aromatase by azole pesticides. SAR QSAR Environ Res, 26 (7-9): 757-782, (2015)
25. B. Webb, A. Sali., Comparative Protein Structure Modeling Using Modeller. Current Protocols in Bioinformatics 54, John Wiley & Sons, Inc., 5.6.1-5.6.37, (2016)
26. Laskowski R A, MacArthur M W, Thornton J M., PROCHECK: validation of protein structure coordinates, in *International Tables of Crystallography, Volume F. Crystallography of Biological Macromolecules*, eds. Rossmann M G & Arnold E, Dordrecht, Kluwer Academic Publishers, The Netherlands, pp. 722-725 (2001)